Available online at www.sciencedirect.com

jmr&t Journal of Materials Research and Technology

journal homepage: www.elsevier.com/locate/jmrt

Original Article

Preparation of ZrB_2 coatings by electrophoretic deposition in NaCl–KCl–$AlCl_3$ molten salts

Chuntao Ge [a], *Qian Kou* [a], *Jie Pang* [a], *Jun Zhang* [b,a], *Weiliang Jin* [a], *Hongmin Zhu* [b,c], *Geir Martin Haarberg* [d], *Saijun Xiao* [a,*]

[a] *School of Metallurgy Engineering, Anhui University of Technology, Maanshan, 243032, China*
[b] *School of Metallurgical and Ecological Engineering, University of Science and Technology Beijing, Beijing, 100083, China*
[c] *Department of Metallurgy, Graduate School of Engineering, Tohoku University, Sendai, 980-8579, Japan*
[d] *Department of Materials Science and Engineering, Norwegian University of Science and Technology, Trondheim, 7491, Norway*

ARTICLE INFO

Article history:
Received 23 May 2022
Accepted 15 July 2022
Available online 19 July 2022

Keywords:
Molten salts Electrophoretic deposition ZrB2 nanoparticles ZrB2 coatings

ABSTRACT

Fabrication of transition metal diboride coatings via electrophoretic deposition in molten salts has been recently proposed, however, the influence of the process parameters on the coating has not yet been studied extensively. In this paper, the effects of cell voltage as well as deposition time on the produced ZrB_2 coatings by electrophoretic deposition of ZrB_2 nanoparticles in NaCl–KCl–$AlCl_3$ molten salts at 710 °C were investigated. The micromorphologies of the surface and the cross-section of the ZrB_2 coatings were characterized by SEM. It was found that with the increase of cell voltage from 1.3 V (i.e., electric field 0.87 V/cm) to 1.8 V (1.2 V/cm), the thickness of the ZrB_2 coating increased under the cell voltages from 1.3 V to 1.5 V and decreased from 1.5 V to 1.8 V. We assume that during the electrophoretic deposition process, the viscosity of molten salt containing high concentration ZrB_2 nanoparticles close to the depositing electrode, which is influenced by the motion rate of nanoparticles governed by the electric field, probably plays an essential role for electrophoretic deposition process of nanoparticles on the electrode. In addition, under the cell voltage of 1.5 V the growth of ZrB_2 coating was studied as a function of deposition time. As the deposition time was increased, the thickness and coherence of the coating were elevated.

1. Introduction

ZrB_2 has excellent comprehensive properties such as high melting point, hardness and wear resistance as well as good thermochemical stability, corrosion resistance, thermal shock resistance, and creep resistance [1–4], so ZrB_2 coatings are widely used for high temperature electrodes [5,6], electrode in plasma applications [7], refractory crucible coatings [8], solar collector plates, surface protection coatings for aerospace and

* Corresponding author.
E-mail address: xiaosaijunzj@yahoo.com (S. Xiao).
https://doi.org/10.1016/j.jmrt.2022.07.095

military armor [9–11]. Over the last decades, they have attracted significant attention from researchers.

The main methods for preparation of ZrB_2 coatings are physical vapor deposition (PVD) [12,13], chemical vapor deposition (CVD) [14], and electroplating in molten salts [15–18]. Among them, the PVD method has a wide range of application, but there are problems such as the inability to precisely control the stoichiometric ratio and the high residual stress of the product [19,20]. For the CVD method, it can achieve precise control of the structure and composition of the coating through the regulation of the deposition process, but the process operation is more complicated, the preparation process is easily contaminated by impurity elements, and more toxic gases are produced [21]. Molten salt electrolysis has advantages of high current efficiency, fast electrolysis, and excellent plating capacity, but it is difficult to obtain compounds with strict component requirements [22]. In addition, ZrB_2 coatings can be prepared by electrophoretic deposition (EPD) [23] in a room temperature solution, which is a low-cost and simple process, and easy to control the coating thickness. However, the product density is so low that it requires additional sintering for densification [24]. It can be seen that there are still many problems to be solved for the preparation of ZrB_2 coatings.

Recently, the present authors have demonstrated the availability of EPD in molten inorganic salts [25,26], and thus proposed a method for the preparation of transition metal boride coatings such as ZrB_2 by EPD in molten salts (i.e., MS-EPD process) [25]. Compared with the conventional preparation method, this process avoids expensive equipment and complicated processes, and the preparation process is environmentally friendly with high product purity. Moreover, the product obtained by MS-EPD process eliminates the densification process compared to EPD in room temperature solutions.

Until now the effects of MS-EPD process parameters on EPDed ZrB_2 coatings in molten salts have not been systematically studied in previous studies. In this paper, the impacts of cell voltage as well as EPD time on the preparation of ZrB_2 coatings by MS-EPD of ZrB_2 nanoparticles in NaCl–KCl–$AlCl_3$ molten salts at 710 °C were investigated.

2. Experimental

2.1. Preparation of nanoparticle-containing solid salts

The NaCl–KCl solid salts containing ZrB_2 nanoparticles were prepared and the preparation process is shown in Fig. 1. A mixture of NaCl (99%, Sinopharm) and KCl (99%, Sinopharm) (1:1 mol, 10 g) with 316 stainless steel balls (φ1 mm: φ3 mm = 3:2 mass, 40 g) were milled in a 316 stainless steel grinding jar for 3 h using a planetary ball mill (HLXPM- φ10X4, Hengle). Then ZrB_2 nanoparticles (mean size 50 nm, 99%, Shanghai ChaoWei Nanotechnology Co. Ltd.) were blended with the milled NaCl–KCl salts at a mass ratio of 1:1, followed by ultrasonic dispersion in acetone for 2 h (100 kHz). Finally, the mixture was dried in a vacuum oven at 120 °C for 1 h.

2.2. Preparation of ZrB_2 coatings by MS-EPD in NaCl–KCl–$AlCl_3$ molten salts

The EPD in NaCl–KCl–$AlCl_3$ molten salts was carried out in an electric resistance furnace with a two-electrode system, under protection of high purity argon for the cell. A DC power supply (HLR-3660D, Henghui) was applied to provide the control of the cell voltage.

Prior to the experiments, NaCl, KCl (heated in advance in a drying oven at 200 °C for more than 48 h) and $AlCl_3$ (99%, Anhydrous, Aladdin) (45:45:10 mol), were introduced into a graphite crucible, heated up to a temperature of 710 °C in an electric resistance furnace. After the mixture was melted sufficiently the electrodes were lowered down into the molten bath. A graphite anode (6*3*50 mm) was immersed into the

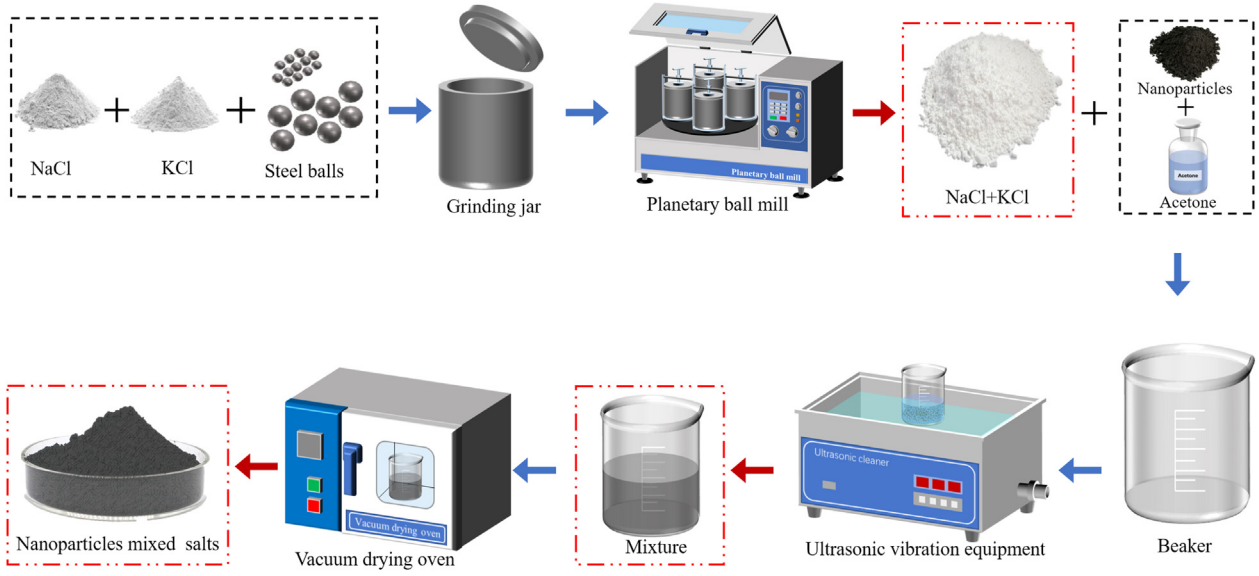

Fig. 1 – Schematic of fabrication of nanoparticles-containing solid salts.

molten salt with a depth of 20 mm, and a graphite cathode (4*1*25 mm) was immersed into the molten salt for 10–15 mm. The distance between the anode and cathode was 15 mm. Pre-electrolysis under 1.5 V cell voltage for 1 h was required to remove some impurities before the conductance of the EPD. Subsequently, the prepared solid salts containing ZrB_2 nanoparticles according to section 2.1 were added to the molten salts through the holes of the upper flange, giving rise to molten NaCl–KCl–$AlCl_3$ containing dispersed ZrB_2 nanoparticles.

Subsequently, the EPD was performed in the molten NaCl–KCl–$AlCl_3$ (45:45:10 mol) system with a ZrB_2 nanoparticle concentration of 40 g/L at an experimental temperature of 710 °C. The applied cell voltages were 1.3 V (i.e., electric field 0.87 V/cm), 1.4 V (0.93 V/cm), 1.5 V (1 V/cm), 1.6 V (1.07 V/cm), 1.7 V (1.13 V/cm) and 1.8 V (1.2 V/cm). The effect of different deposition time (7 min, 10 min, 20 min, 30 min and 60 min) on the ZrB_2 coating was investigated with a ZrB_2 nanoparticle content of 50 g/L. After the deposition, the cathode was removed and cleaned by soaking in deionized water for 1 h, followed by drying and characterization.

2.3. *Characterization*

The surface and cross-sectional morphologies of the EPDed ZrB_2 coatings were examined using a scanning electron microscopy (SEM) (Regulus 8220, HITACHI and JSM-6510, JEOL). X-ray diffraction (XRD) (Smart Lab, Rigaku, voltage: 40 kV, current: 40 mA, scan rate: 10°/min) was used to analyze their phase composition.

3. Results and discussion

3.1. *Effect of cell voltage on the EPDed ZrB_2 coatings*

In NaCl–KCl–$AlCl_3$ molten salts at 710 °C, cell voltages of 1.3–1.8 V were applied to perform the MS-EPD of ZrB_2 nanoparticles on graphite cathodes for 1 h. Fig. 2a gives the photographs of the EPDed coatings. It can be obviously observed that there was a deposit on all the graphite plates. The typical result of the XRD analysis for those deposits, as shown in Fig. 2b, indicates that it was pure ZrB_2.

The surface morphologies of the ZrB_2 deposits fabricated by MS-EPD process under 1.3–1.8 V were characterized by SEM as shown in Fig. 3. When the cell voltage was 1.3 V (Fig. 3a), the surface of the coating was continuous and free of holes, consisting of a large amount of aggregates with an average size of around 3 μm. It could be seen that the aggregates were composed of individual particles (top-right inset of Fig. 3a), which were of nanoscale size, under higher magnification as shown in Fig. 3a. With increased cell voltages of 1.4 V and 1.5 V, the average sizes of the aggregates composing the surface increased to around 5 μm and 10 μm, respectively (Fig. 3b, c). The aggregates still consisted of nanoparticles (Fig. 3b, c). However, with continuously enhanced cell voltage of 1.6 V, the average size of the aggregates decreased to about 4 μm (Fig. 3d). As the cell voltage was further increased to 1.7 V and 1.8 V, the coating appeared to be flatter than that at 1.5 V and 1.6 V. The presence of the aggregates was identified with decreased averaged sizes of around 1 μm and below 1 μm, respectively. Under cell voltages of 1.6–1.8 V, the aggregates were also composed of nanoscale particles (Fig. 3d, e, f). The results show that the influence of the cell voltage on the surface morphology of ZrB_2 coatings is that the size of the aggregates on the surface increased with increasing cell voltages from 1.3 V to 1.5 V and decreased from 1.5 V to 1.8 V. Under all the applied cell voltages (1.3–1.8 V), all the ZrB_2 aggregates consisted of nanoscale particles.

The SEM images of the fractured cross-section of the obtained ZrB_2 coatings under 1.3–1.8 V are shown in Fig. 4. When the cell voltage was 1.3 V, a dense coating with a thickness of around 3 μm was prepared, which was well bonded to the substrate without peeling. The surface consisted of spherical aggregates with an average size of around 3 μm, which corresponded to the characterization results for its surface morphology. With increased cell voltages of 1.4 V and 1.5 V, the thickness of the coatings increased to about 6 μm and 15 μm, respectively, which tended to be more uniform and coherent. The average sizes of the aggregates composing the coating surface increased to about 5 μm and 10 μm,

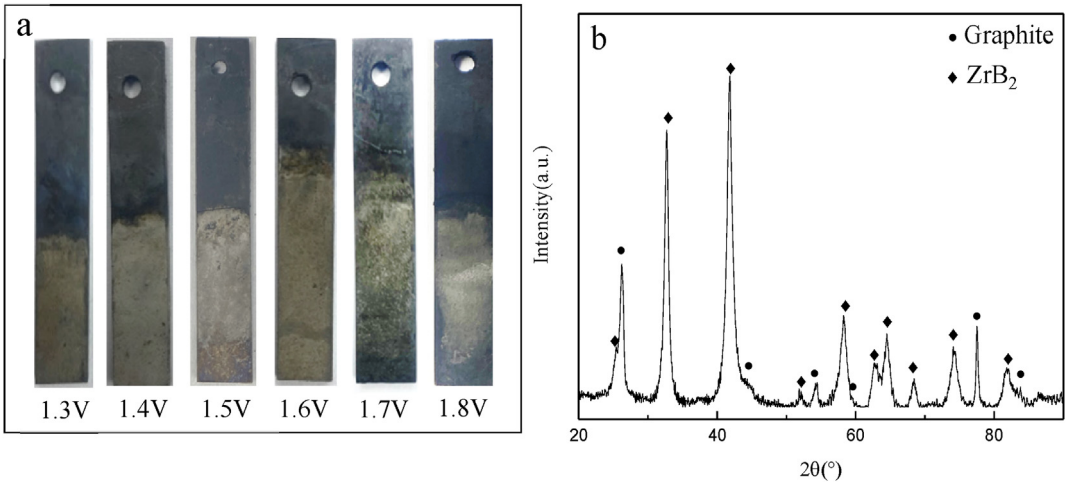

Fig. 2 – Photographs of the EPDed coatings under cell voltages of 1.3–1.8 V (a) and typical XRD characterization (b) of the deposits on graphite cathodes in NaCl–KCl–$AlCl_3$ melt at 710 °C for 1 h.

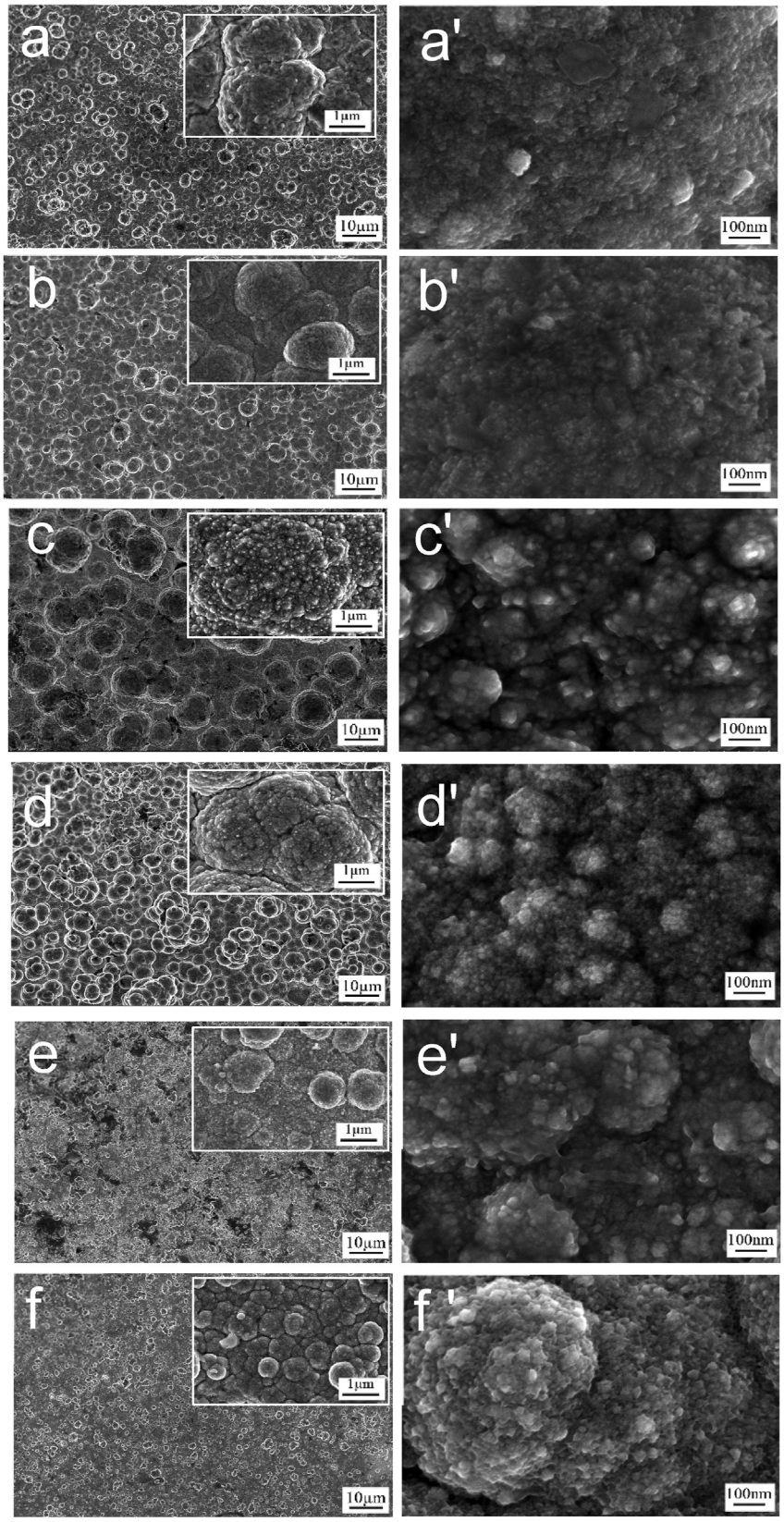

Fig. 3 – The SEM images of the surface of the EPDed ZrB_2 coatings on graphite substrates under 1.3–1.8 V for 1 h with a ZrB_2 nanoparticle concentration of 40 g/L in NaCl–KCl–$AlCl_3$ melt at 710 °C (a. 1.3 V; b. 1.4 V; c. 1.5 V; d. 1.6 V; e. 1.7 V; f. 1.8 V).

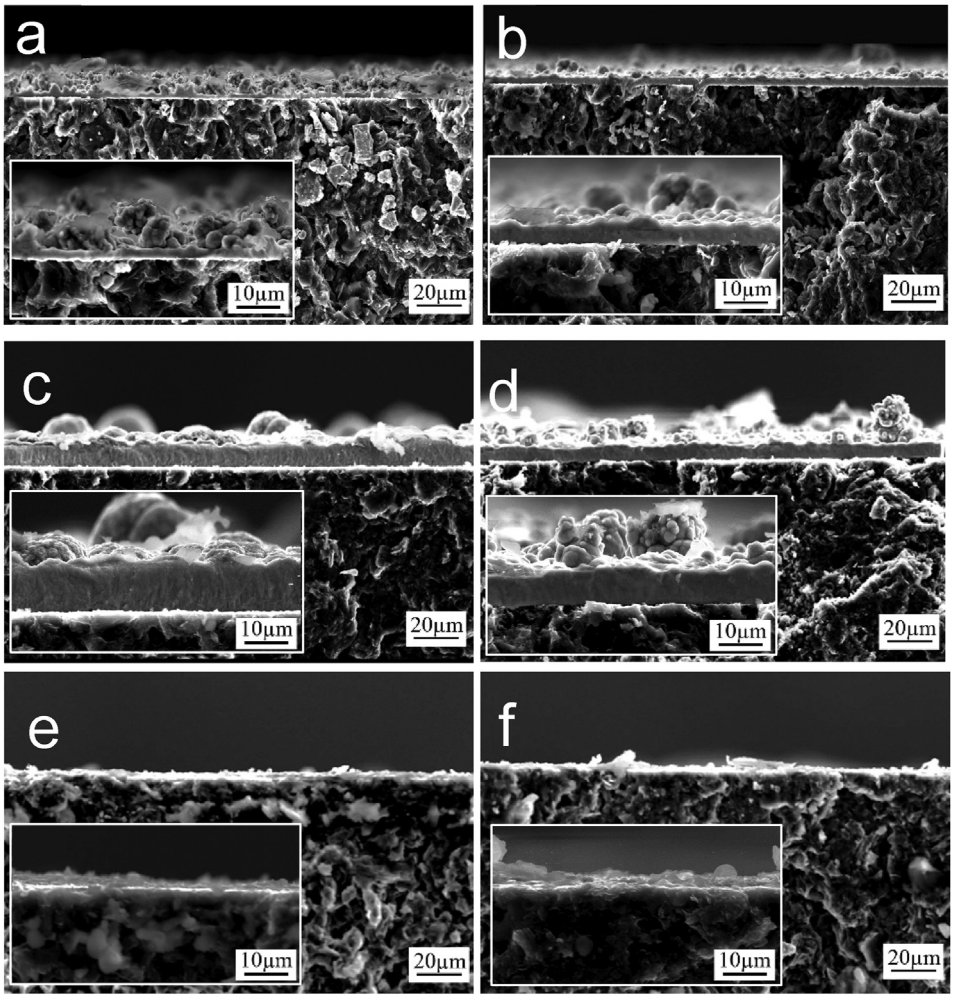

Fig. 4 – The SEM images of the fractured cross-section of the EPDed ZrB_2 coatings on graphite substrates under 1.3–1.8 V for 1 h with a ZrB_2 concentration of 40 g/L in NaCl–KCl–$AlCl_3$ melt at 710 °C (a. 1.3 V; b. 1.4 V; c. 1.5 V; d. 1.6 V; e. 1.7 V; f. 1.8 V).

respectively, but the amounts were reduced (Fig. 4b, c). After the cell voltage was increased to 1.6 V, the coating thickness decreased to about 10 μm. The average size of the spherical aggregates comprising the coating surface decreased to about 4 μm, and their amount increased instead. With continuously increased cell voltages of 1.7 V and 1.8 V, the coating thickness dropped sharply and the aggregates could not be observed obviously.

It has been considered that during the EPD process in aqueous or organic suspensions, the nanoparticles migrate and approach the electrode under the effect of an electric field, causing the concentration of nanoparticles near the cathode to increase, and then they continue to move and deposit on the electrode from the suspension with high nanoparticle concentration near the electrode, resulting in a deposited layer with a uniform structure [27]. It has been also reported that the behavior of the deposited layer is similar to that of a viscous fluid in ethanol suspensions [28]. In the present investigation, it is assumed that during the MS-EPD process there also exists a layer of viscous fluid in the vicinity of the depositing electrode and based on the above results of SEM analysis for the ZrB_2 coating, we attempt to illustrate the migration and deposition behavior of nanoparticles during the MS-EPD process, as shown in Fig. 5. The presence of three layers close to the depositing electrode is suggested and demonstrated, including a layer of viscous fluid, i.e., molten salts with higher concentration of nanoparticles than that in the bulk, a layer of coherent coating bonding well with the cathode substrate and a transition layer consisting of aggregates mixed with a small amount of viscous fluid. When the MS-EPD of nanoparticles begins under an electric field, a layer of viscous fluid was formed, which simultaneously supply the nanoparticles to form aggregates in the transition layer. At the same time, with continuously accumulation of nanoparticles in the transition layer, it was transformed into a coherent layer. As the MS-EPD process proceeds, the coherent layer gradually becomes thicker, giving rise to a compact and coherent coating.

In the present study, with a small cell voltage, the ZrB_2 nanoparticles migrate slowly and it takes longer time to reach the cathode. The concentration of nanoparticles near the cathode is relatively low, leading to a lower probability of nanoparticle aggregation, so the aggregates in the transition layer are smaller in size but relatively larger in number. At the same time, the low transformation rate of the ZrB_2 aggregates to be the coherent layer also results in a relatively thin ZrB_2 coating. As the cell voltage is increased from 1.3 V to 1.5 V, the

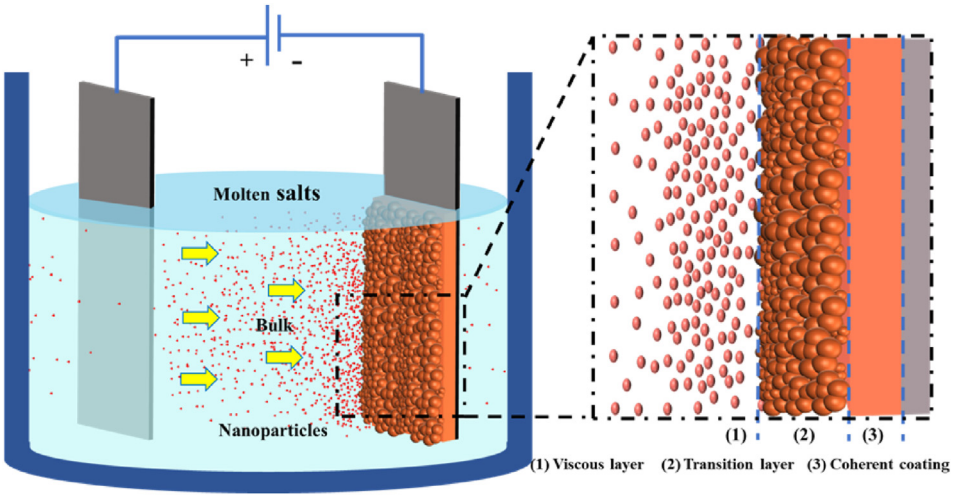

Fig. 5 – Schematic drawing of migration and deposition behavior of nanoparticles in molten salts under an electric field during the MS-EPD process.

movement of nanoparticles accelerates, thus the concentration of nanoparticles in the vicinity of the cathode increases, resulting in ZrB_2 aggregates with a larger size and a reduced amount and more uniform and thicker ZrB_2 coatings [29,30]. However, the continuous increase of cell voltage (1.6–1.8 V) leads to more amount of ZrB_2 aggregates with smaller size and thinner thickness of the ZrB_2 coating instead. We assume that the viscosity of the viscous fluid continuously increases with the elevated speed of nanoparticle migration caused by the enhancement of the cell voltage. In this case, the fast motion of the ZrB_2 nanoparticles (e.g., under the cell voltage of 1.6–1.8 V) probably causes a too high viscosity of the viscous fluid layer, which, instead, hinders the movement of nanoparticles to the transition layer and thus prevents the normal deposition process, leading to ZrB_2 aggregates with a smaller size and a larger amount and reduced thickness of the ZrB_2 coating. It is noted that when the cell voltage is further increased to 1.7–1.8 V, we assume that the viscosity of the viscous layer probably increases rapidly at the early stage of the deposition, thus preventing the effective supply of ZrB_2 nanoparticles at the initial stage, resulting in a significant decrease in the thickness of the deposited layer.

In summary, ZrB_2 coatings could be produced by MS-EPD under cell voltages of 1.3–1.8 V in molten NaCl–KCl–$AlCl_3$ system, and the cell voltage has as obvious impact on the surface and cross-section morphologies of the obtained ZrB_2 coatings. It is considered that the variation of cell voltage leads to a change of the viscosity of the viscous fluid layer, which significantly influenced the mass transfer of the ZrB_2 nanoparticles, thus their deposition behavior. It is suggested the cell voltage of 1.5 V is the optimized value, resulting in suitable viscosity of the viscous fluid layer, which favors the mass transfer and MS-EPD of ZrB_2 nanoparticles.

3.2. *Effect of deposition time on the EPDed ZrB_2 coatings*

The EPDed ZrB_2 coatings obtained for varied deposition time of 7–60 min under a cell voltage of 1.5 V in NaCl–KCl–$AlCl_3$ melt at 710 °C were studied to investigate the growth process. The surface SEM images of the products are shown in Fig. 6, and the cross-sectional SEM images are shown in Fig. 7. With the deposition time of 7 min, a ZrB_2 coating appeared on the cathode surface, but there were some holes on the surface (Fig. 6a). ZrB_2 aggregates with an average size of about 400 nm were observed after magnification (top-right inset in Fig. 6a). Further magnification revealed that the size of the particles consisting of the aggregates reached a nanometer level. From the corresponding cross-sectional image (Fig. 7a), the thickness of the coating was nearly 2 μm, which spread over the whole substrate. With the deposition time of 10 min, the holes on the surface were filled with tiny particles (Fig. 6b). The average size of the aggregates grew up to about 1 μm as seen in the larger magnification image (top-right inset of Fig. 6b). In Fig. 7b the coating thickness increased slightly, and the surface of the substrate was fully covered by the dense film. By increasing the time to 20 min, the holes on the surface almost disappeared, and the aggregates grew up to about 2 μm in size (Fig. 6c). The thickness of the coating increased to about 5 μm (Fig. 7c). In this case, the existence of ZrB_2 aggregates from the view of the cross-section of the coating could be clearly observed. When the deposition time was 30 min, the coating surface was continuous without holes (Fig. 6d). The aggregates composing the surface were around 5 μm in size. In the SEM images of the cross-section (Fig. 7d), the thickness growth of the coating was not obvious, with more amount of aggregates on it. After the deposition time was up to 60 min, the average ZrB_2 aggregate size was about 10 μm (Fig. 6e). The thickness of the coating increased to about 15 μm (Fig. 7e), which was uniform and dense. In addition, from 7 min to 60 min, the ZrB_2 aggregates consisting of the surface of the coatings were made up of nanoparticles (Fig. 6a-e). As the deposition time was increased, the thickness of the coating increased and the size of the ZrB_2 aggregates comprising the coating surface became larger.

It is known that in the process of EPD, nanoparticles move under the effect of electric field to approach the depositing electrode and the deposition amount increases with the deposition time [31,32]. According to the illustration of migration and deposition behavior of nanoparticles

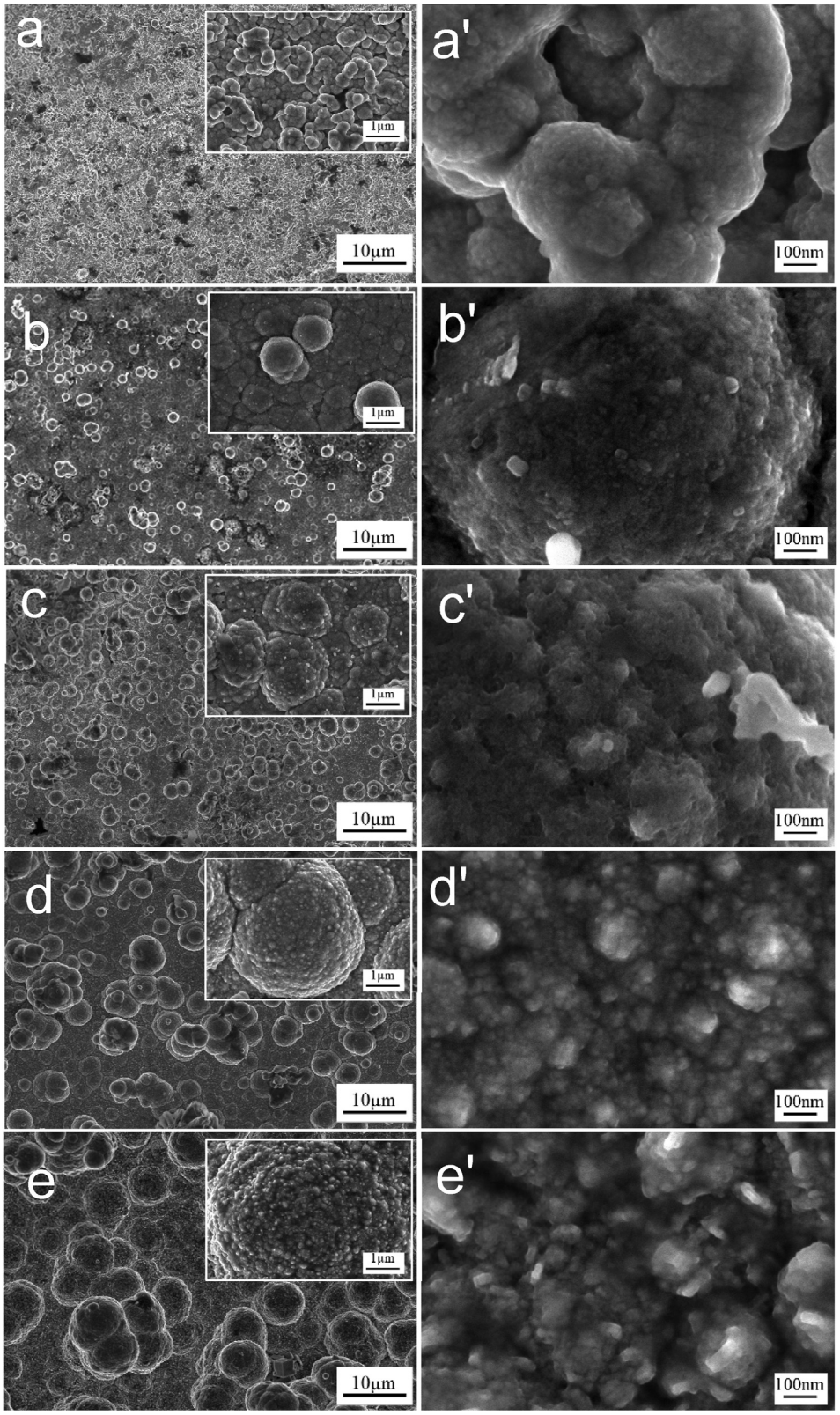

Fig. 6 – The SEM images of the surface of the EPDed ZrB_2 coating on graphite substrates for 7–60 min under 1.5 V with a ZrB_2 concentration of 50 g/L in NaCl–KCl–$AlCl_3$ melt at 710 °C (a. 7 min; b. 10 min; c. 20 min; d. 30 min; e. 60 min).

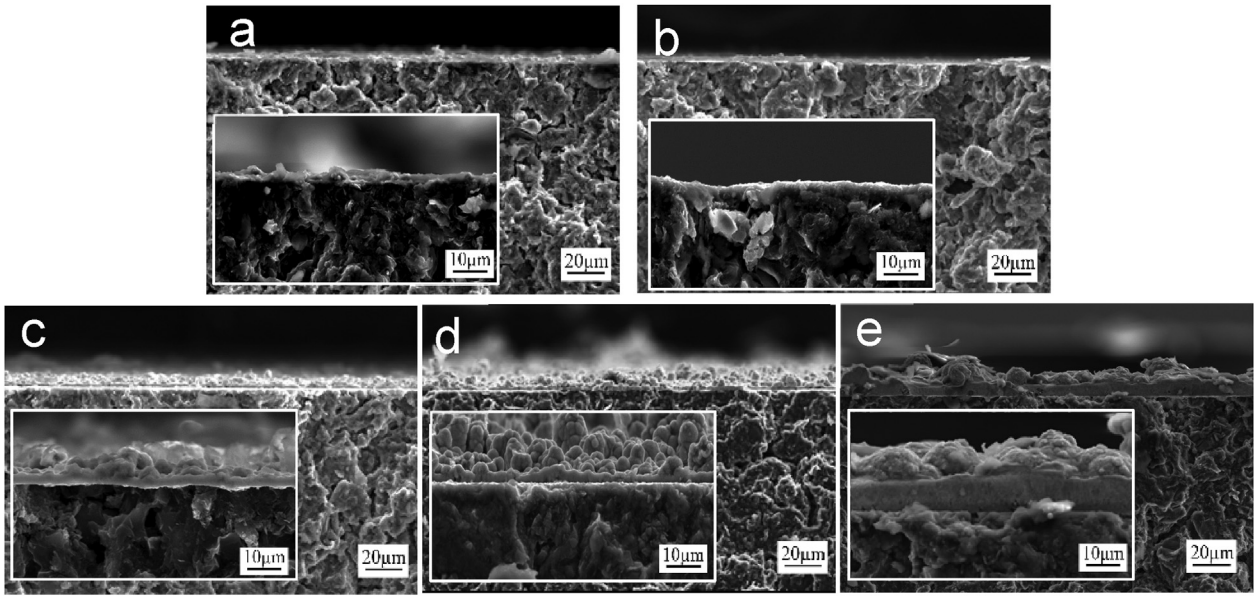

Fig. 7 – The SEM images of the fractured cross-section of the EPDed ZrB_2 coatings on graphite substrates for 7–60 min under 1.5 V with a ZrB_2 concentration of 50 g/L in NaCl–KCl–$AlCl_3$ melt at 710 °C (a. 7 min; b. 10 min; c. 20 min; d. 30 min; e. 60 min).

mentioned in section 3.1, as shown in Fig. 5, at the early stage of the MS-EPD of ZrB_2 nanoparticles, the number of nanoparticles close to the cathode is relatively low, with a small chance of agglomerating, giving rise to aggregates which are smaller in size, resulting in a relatively low transformation of aggregates to the coherent layer and relatively thin thickness of the coating. As time increases, the continuous supply of nanoparticles brings the concentration of nanoparticles near the cathode to be greater, and the size of the aggregates becomes bigger, which facilitating the transformation of aggregates to be the coherent layer, leading to an enhancement of the thickness of the coating. Therefore, it is evident that the deposition time affects the size of the ZrB_2 aggregates comprising the surface of the coating and the thickness of the coating. With the increase of time, the EPDed ZrB_2 coating becomes more coherent and thicker.

4. Conclusions

The effects of cell voltage (1.3–1.8 V) and deposition time (7–60 min) on the ZrB_2 coatings, prepared by MS-EPD of ZrB_2 nanoparticles in NaCl–KCl–$AlCl_3$ melt at 710 °C, have been studied. The main conclusions are as follows.

(1) ZrB_2 coatings can be obtained by MS-EPD under the cell voltages of 1.3–1.8 V in NaCl–KCl–$AlCl_3$ molten salts.
(2) From 1.3 V to 1.8 V, the cell voltage affects the morphology of the surface and the thickness of the coating. The size of ZrB_2 aggregates composing the coating surface gradually increases from 1.3 V to 1.5 V and decreases from 1.5 V to 1.8 V. The thickness of the coating also rises from 1.3 V to 1.5 V and drops from 1.5 V to 1.8 V. It is suggested that during the MS-EPD process, the variation of cell voltage, essentially causes the change of the viscosity of molten salts including high ZrB_2 nanoparticles in the vicinity of the cathode, which has a significant effect on the MS-EPD process. It is considered that the cell voltage of 1.5 V (i.e., electric field 1 V/cm) is the optimized value, resulting in suitable viscosity of the viscous fluid layer, which favors the mass transfer and MS-EPD of ZrB_2 nanoparticles.
(3) At the cell voltage of 1.5 V, as the deposition time increases from 7 min to 60 min, the size of the ZrB_2 aggregates consisting of the coating surface rises and the thickness of the coating is enhanced, due to more accumulating of ZrB_2 nanoparticles in the viscous layer and more transformation of ZrB_2 aggregates to be the coherent layer.

Declaration of Competing Interest

The authors declare that they have no known competing financial interests or personal relationships that could have appeared to influence the work reported in this paper.

REFERENCES

[1] Zhang XH, Hu P, Han JC, Meng SH, Du SY. Research progress on ultra-high temperature ceramic composites. Chin Sci Bull 2015;60:257–66.
[2] Das J, Kesava BC, Reddy JJ, Srinivas V, Kumari S, Prasad VB, et al. Microstructure, mechanical properties and oxidation behavior of short carbon fiber reinforced ZrB_2-20v/oSiC-2v/oB_4C composite. Mater Sci Eng, A 2018;719:206–26.
[3] Kiryukhantsev-Korneev P, Sytchenko A, Kaplanskii Y, Sheveyko A, Vorotilo S, Levashov E. Structure, corrosion

resistance, mechanical and tribological properties of ZrB_2 and Zr-B-N coatings. Metals 2021;11:1194.
[4] Kiryukhantsev-Korneev FV, Lemesheva MV, Shvyndina NV, Levashov EA, Potanin AY. Structure, mechanical properties, and oxidation resistance of ZrB_2, ZrSiB, and ZrSiB/SiBC coatings. Prot Met Phys Chem Surf 2018;54:1147–56.
[5] Jung SH, Oh HC, Kim JH, Choi SC, Lee SH, Kim HD. Pretreatment of zirconium diboride powder to improve densification. J Alloys Compd 2013;548(1):173–9.
[6] Khanra AK, Sarkar BR, Bhattacharya B, Pathak LC, Godkhindi MM. Performance of ZrB_2–Cu composite as an EDM electrode. J Mater Process Technol 2007;183(1):122–6.
[7] Norasetthekul S, Eubank PT, Bradley WL, Bozkurt B, Stucker B. Use of zirconium diboride copper as an electrode in plasma applications. J Mater Sci 1999;34(6):1261–70.
[8] He ZY, NPeng XY, Li L, Liu KQ. Effect of ZrB_2 on oxidation resistance of low-carbon MgO-C materials. Refract 2006;40:280–2.
[9] Opeka MM, Talmy IG, Zaykoski JA. Oxidation-based materials selection for 2000°C hypersonic aero surfaces: theoretical considerations and historical experience. J Mater Sci 2004;39(19):5887–904.
[10] Liu CQ, Li KZ, Li HJ, Zhang SY, Zhang YL. In situ synthesis mechanism of ZrB_2-ZrC-C composites. Ceram Int 2014;40(7):10297–302.
[11] Vajdi M, Moghanlou FS, Niari ER, Asl MS, Shokouhimehr M. Heat transfer and pressure drop in a ZrB_2 microchannel heat sink: a numerical approach. Ceram Int 2019;46:1730–5.
[12] Samuelsson M, Jensen J, Helmersson U, Hultman L, Högberg H. ZrB_2 thin films grown by high power impulse magnetron sputtering from a compound target. Thin Solid Films 2012;526:163–7.
[13] Bera S, Sumiyoshi Y, Yamada-Takamura Y. Growth of single-crystalline zirconium diboride thin film on sapphire. J Appl Phys 2009;106(6):063531.
[14] Souqui L, Palisaitis J, Ghafoor N, Pedersen H, Högberg H. Rhombohedral boron nitride epitaxy on ZrB_2. J Vac Sci Technol, A 2021;39:013405.
[15] Anthony KE, Welch BJ. Electrodeposition of zirconium diboride from oxides dissolved in fused salts. Aust J Chem 1969;22:1593–7.
[16] Mellors GW, Senderrofif S. Electrodeposition of coherent coatings of refractory metals: VII. zirconium diboride. J Electrochem Soc 1971;118:220–5.
[17] Uskova NN, Sarychev SY, Malyshev VV, Shapoval VI. High-temperature electrochemical synthesis of zirconium diboride in halogenide. Zh Prikl Khim 2000;73:1456–61.
[18] Wang Q, Wang YL, Liu HJ, Zeng CL. Electrochemical deposition of zirconium diboride coatings in NaCl-KCl-K_2ZrF_6-KBF_4 melts. J Electrochem Soc 2016;163(10):636–44.
[19] Berger M, Larsson M, Hogmark S. Evaluation of magnetron-sputtered TiB_2 intended for tribological applications. Surf Coat Technol 2000;124(2):253–61.
[20] Mitterer C, Rauter M, Rödhammer P. Sputter deposition of ultrahard coatings within the system Ti-B-C-N. Surf Coat Technol 1990;41(3):351–63.
[21] Zhang L, Li GD, Xiong X, Zhang J. Effect of reactive gas on the phase and microstructure of ZrB_2 coating. Mater Sci Eng Powder Meta llurgy 2017;3:335–41.
[22] Wang Q, Zhang L, Liu HJ, Zeng CL. Review on preparation of ZrB_2 by electrodeposition in molten salts. Corros Sci Prot Tech 2018;30:87–94. 02.
[23] Dong ZH, Peng X, Wang FH. Oxidation of a ZrB_2 coating fabricated on Ta–W alloy by electrophoretic deposition and laser melting. Mater Lett 2015;148(1):76–8.
[24] Zhang QH. Research progress of nano-ceramic. Surf Technol 2017;46(5):215–23.
[25] Jin WL, Xiao SJ, Kou Q, Ding DS, Zhang J, Fang XH, et al. Preparation of diboride coatings by electrophoretic deposition in nanoparticle containing molten inorganic salts. Mater Lett 2022;306:130908.
[26] Zhang J, Chu SJ, Jin WL, Cai F, Zhu HM, Xiao SJ. Fabrication of TiB_2 coatings by electrophoretic deposition of synthesized TiB_2 nanoparticles in molten salt. J Mater Res Technol 2022;18:2451–7.
[27] Hamaker HC, Verwey EJW. The role of the forces between the particles in electrodeposition and other phenomena. Trans Farad Soc 1940;36:180–5.
[28] Sarkar P, Nicholson PS. Electrophoretic deposition (EPD): mechanisms, kinetics, and application to ceramics. J Am Ceram Soc 1996;79(8):1987–2002.
[29] Sussman A, Ward TJ. Elecmophoretic deposition of coatings from lassanols. RCA Rev 1981;42:178–97.
[30] Yang SK, Cai WP, Liu GQ, Zen HB. From nanoparticles to nanoplates: preferential oriented connection of Ag colloids during electrophoretic deposition. J Phys Chem C 2009;113:7692–6.
[31] Xua LH, Kajiyoshi K, Yan YW. Preparation of highly oriented titania nanosheet thin films by electrophoretic deposition. Thin Solid Films 2009;518:10–5.
[32] Nicholson PS, Sarkar P, Haung X. Electrophoretic deposition and its use to synthesize ZrO_2/Al_2O_3 micro-laminate ceramic/ceramic composites. J Mater Sci 1993;28:6274–8.